Synthesis of deuterium-labelled amlexanox and its metabolic stability against mouse, rat and human microsomes

Xinmin Gan[a,b], Michael W. Wilson[a,b], Tyler S. Beyett[c,d], Bo Wen[e], Duxin Sun[e], Scott D. Larsen[a,b], John J. G. Tesmer[f], Alan R. Saltiel[g] and Hollis D. Showalter[a,b*]

[a]Department of Medicinal Chemistry, [b]Vahlteich Medicinal Chemistry Core, [c]Program in Chemical Biology, [d]Life Sciences Institute, Departments of Pharmacology and Biological Chemistry, [e]Department of Pharmaceutical Sciences, University of Michigan, Ann Arbor, MI 48109, United States

[f]Departments of Biological Sciences and Medicinal Chemistry and Molecular Pharmacology, Purdue University, West Lafayette, IN 47907-2054

[g]Departments of Medicine and Pharmacology, Institute for Diabetes and Metabolic Health, University of California, San Diego, La Jolla, CA 92093-0912, United States

*Corresponding author

Abstract: As part of a program toward making analogues of amlexanox (**1**), currently under clinical investigation for the treatment of type 2 diabetes and obesity, we have synthesized derivative **5** in which deuterium has been introduced into two sites of metabolism on the C-7 isopropyl function of amlexanox. The synthesis of **5** was completed in an efficient three-step process utilizing reduction of key olefin **7b** to **8** by Wilkinson's catalyst to provide specific incorporation of di-deuterium across the double bond. Compound **5** displayed nearly equivalent potency to amlexanox (IC$_{50}$ 1.1 µM vs 0.6 µM, respectively) against recombinant human TBK1. When incubated with human, rat, and mouse liver microsomes, amlexanox (**1**) and d_2-amlexanox
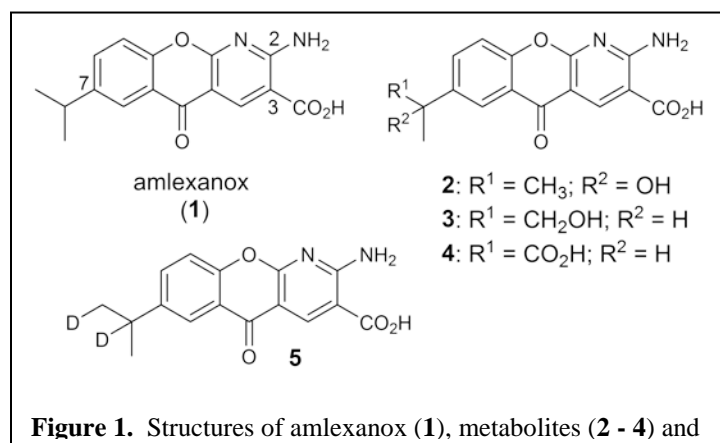
(**5**) were stable (t$_{1/2}$ > 60 min) with **1** showing marginally greater stability relative to **5** except for rat liver microsomes. These data show that incorporating deuterium into two sites of metabolism does not majorly suppress Cyp-mediated metabolism relative to amlexanox.

1.   INTRODUCTION

There is currently a worldwide epidemic of obesity, which is manifesting itself as a leading risk factor in industrialized countries for the development of type 2 diabetes, dyslipidaemia, non-alcoholic fatty liver disease, cardiovascular disease and some cancers.[1] Obesity results from a sustained imbalance between calorie intake and energy expenditure and is characterized by chronic, low-grade inflammation in liver and adipose tissues, which in turn attenuates the actions of multiple hormones to produce a dysregulated metabolic state.[2,3,4] Prior studies on the role of inflammation in the generation of insulin resistance and type 2 diabetes during obesity implicate an important role for the nuclear factor kappa-light-chain-enhancer of activated B cells (NF-κB) pathway, revealing the role of two non-canonical inhibitors of kappa B (IκB) kinases, TANK-binding kinase 1 (TBK1) and inhibitor of nuclear factor kappa-B kinase subunit ε (IKKε), in insulin-independent pathways that promote energy storage and block adaptive energy expenditure during obesity.[5,6] Since none of the currently available and widely used treatments for obesity addresses the underlying energy imbalance associated with inflammation pathways,[7] we initiated a high throughput screen for small molecule inhibitors of the TBK1 and IKKε kinases. One hit from our screen was amlexanox (**1**; Figure 1), an approved drug developed by Takeda that is used for the treatment of canker sores, asthma, and allergic rhinitis.[8,9] The compound is a modest inhibitor of TBK1 and IKKε and reproduced the effects of the IKKε knockout phenotype, which include weight loss in obese mice, improved insulin sensitivity, and reduced hepatic steatosis and inflammation. Amlexanox also increased the level of the second messenger molecule cAMP and triggered the release of the hormone interleukin-6 (IL-6) from fat cells thereby reducing the production of glucose. Two recent clinical trials indicated that amlexanox treatment effectively lowered glycated hemoglobin


Figure 1. Structures of amlexanox (**1**), metabolites (**2 - 4**) and

(HbA1c) in a subset of patients with obesity and type 2 diabetes.[10] Despite these promising results, the future utility of amlexanox in the clinic for obesity and type 2 diabetes intervention may be limited by its solubility, modest potency, and/or metabolic profile.

Previous studies by Takeda investigators showed that the oral administration of amlexanox (**1**) in mice, rats, guinea pigs, and dogs generated in plasma a major mono-hydroxyl metabolite (**2**) from oxidation of the C-7 isopropyl substituent, and two minor metabolites **3** and **4**[11,12] (Figure 1). The glucuronide of **1** was also identified in rats. In humans, the main metabolite was **2**. The structures of metabolites **2** and **3** have been confirmed by synthesis.[13]

As part of a program toward making analogues of amlexanox,[14,15] we decided to synthesize a derivative **5** (Figure 1) in which deuterium is introduced into two sites of metabolism on the C-7 isopropyl function. The deuterium kinetic isotope effect associated with placing deuterium at the site of metabolic derivatization slows metabolic activation and thus is expected to increase the lifetime of the active drug in vivo.[16] Herein we provide data of the activity of **5** relative to amlexanox (**1**) in inhibiting TBK1 and its metabolic stability against mouse, rat and human microsomes.

2. RESULTS AND DISCUSSION

Synthetic chemistry. Initial approaches toward generating d_1-amlexanox, in which the benzylic C-7 methine was exchanged for deuterium, centered on

Scheme 1. Synthesis of d_2-amlexanox (**5**)
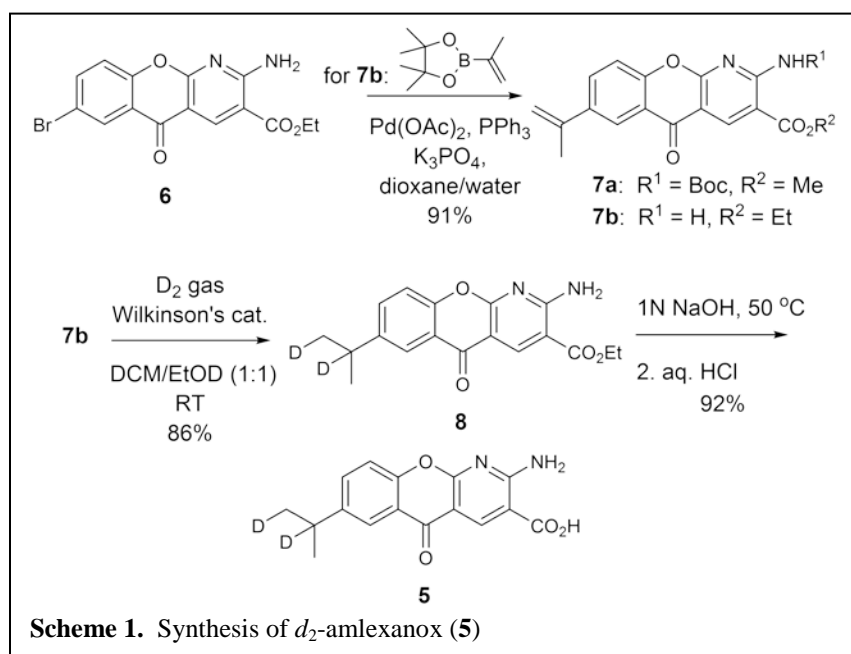
catalytic exchange chemistry. Thus, reaction of amlexanox (**1**) under a variety of conditions (hydrogen gas, 10 – 30% palladium on activated carbon, methanol-d_4, 25-50 °C) left starting material only. We then focused on incorporation of deuterium through room temperature hydrogenation of the olefin in compound **7a**, made by known procedures,[13,17] with deuterium gas in the presence of 10% palladium on activated carbon in ethyl acetate. Thus, a control reduction of **7a** with hydrogen gave cleanly the non-deuterated C-7 isopropyl product. Substitution of deuterium for hydrogen gas yielded a new set of products with mass spectrum peaks associated with incorporation of more than two atoms of deuterium. The ^{1}H NMR spectrum suggested that the predominant *N*-Boc carboxylic methyl ester product had incorporated four atoms of deuterium and ^{13}C NMR experiments on the next step hydrolysis product (analogous to **5**) indicated the presence of seven uniquely substituted C-7 methine carbons. This showed that deuterium had been incorporated non-specifically into both C-7 methyl groups as well as the methine carbon. There is literature precedence for such scrambling of isotopic incorporation into benzylic and allylic sites.[18]

After unsuccessfully surveying other heterogenous catalytic conditions, we then resorted to olefin reduction with a homogeneous catalyst (Scheme 1). Employing our recently published methodology of introducing C-7 substituents via late-stage coupling chemistry to make amlexanox analogues[15], we reacted tricyclic bromide **6**[19] with 2-propenyl pinacol boronic ester under standard Suzuki coupling conditions to give **7b** in 91% yield. Reaction with

tris(triphenylphosphine)rhodium(I) chloride (Wilkinson's catalyst) and deuterium gas, as previously described for similar reductions,[20,21] proceeded in high yield to give key intermediate **8** with specific incorporation of di-deuterium across the double bond. Standard hydrolysis conditions as described before[15] then provided d_2-amlexanox (**5**) in 92% yield and 72% overall yield from starting ester **6**. All compounds were rigorously purified by
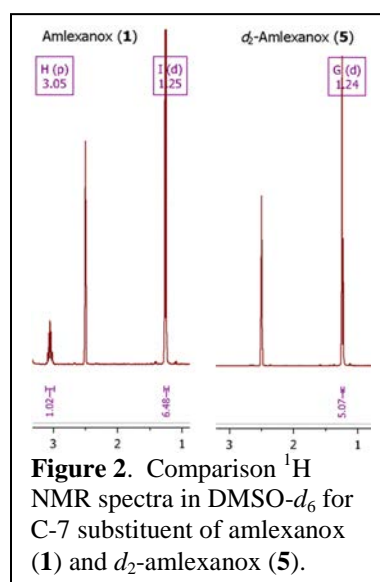
Figure 2. Comparison ^{1}H NMR spectra in DMSO-d_6 for C-7 substituent of amlexanox (**1**) and d_2-amlexanox (**5**).

flash chromatography or crystallization, and their structural assignments are supported by diagnostic peaks in the ^{1}H and ^{13}C NMR spectra and by high resolution mass spectrometry. Digital copies of NMR and mass spectra can be found in Supplementary Materials Online.

The ^{1}H NMR spectra of the upfield region (δ 1-3 ppm) for the C-7 isopropyl substituent (Figure 2) clearly show clean, specific incorporation of di-deuterium into **5**. Complete collapse of the symmetrical pentet at δ 3.05 ppm occurs in **1** and the symmetrical doublet at δ 1.25 ppm, integrating for six protons, changes to an unsymmetrical doublet in **5** integrating for five protons. High resolution mass spectra for **5** and **8** (Supplementary Materials Online) also support specific incorporation of di-deuterium.
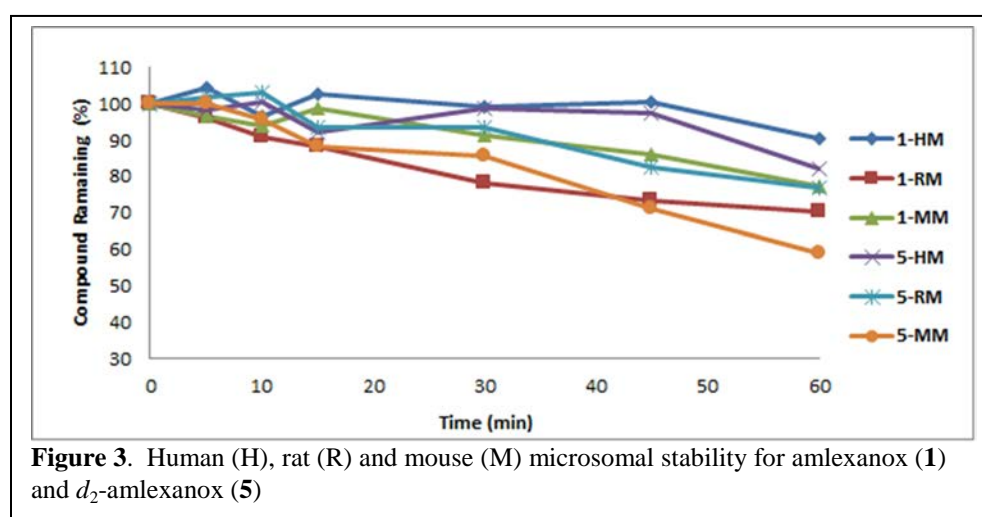
Figure 3. Human (H), rat (R) and mouse (M) microsomal stability for amlexanox (**1**) and d_2-amlexanox (**5**)

Metabolic stability studies. Amlexanox (**1**) and d_2-amlexanox (**5**) are moderately metabolized by human, rat and mice liver microsomes. The in vitro disappearance half-life ($t_{1/2}$) of both compounds in all three microsomes is over 60 min (Figure 3). During the incubation in human and mice liver microsomes, about 8% more unmetabolized amlexanox remains after 60 min compared to d_2-amlexanox. However, d_2-amlexanox (**5**) is more stable than amlexanox (**1**) in rat liver microsomes. Both compounds show greater stability in human liver microsomes relative to the other microsomes. Verapamil was employed as positive control compound in order to ensure that the microsomes and NADPH used in this study were active and that incubation conditions
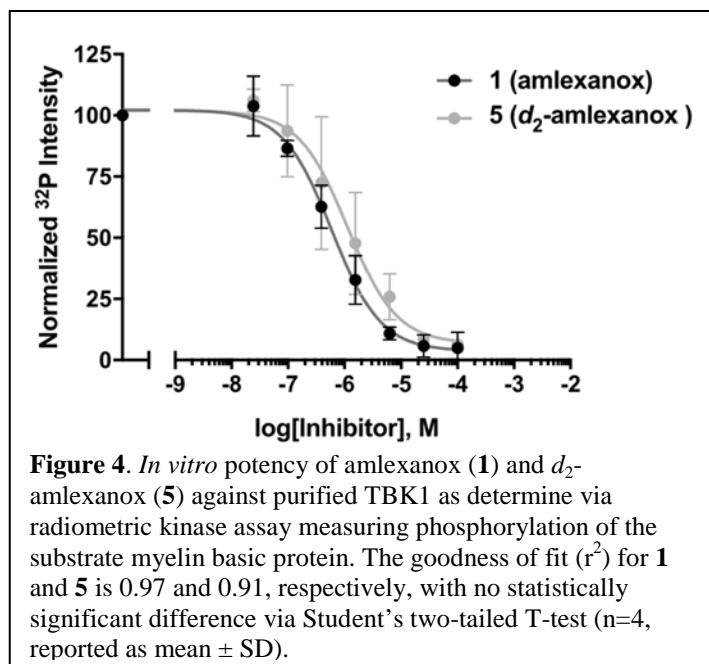
were appropriate to perform the studies. Based on the observed degradation patterns, amlexanox (**1**) and d_2-amlexanox (**5**) are considered to be stable against the three liver microsomes.

<u>Activity against TBK1 kinase</u>. d_2-Amlexanox (**5**) was investigated for inhibition of recombinant human TBK1 as described previously.[15] The IC_{50} values shown were determined by dose-response radiometric kinase assays with

Figure 4. *In vitro* potency of amlexanox (**1**) and d_2-amlexanox (**5**) against purified TBK1 as determine via radiometric kinase assay measuring phosphorylation of the substrate myelin basic protein. The goodness of fit (r^2) for **1** and **5** is 0.97 and 0.91, respectively, with no statistically significant difference via Student's two-tailed T-test (n=4, reported as mean ± SD).

myelin basic protein as substrate, and are technically apparent IC_{50} values. Each is an average of three separate determinations. Since the isopropyl group on amlexanox is solvent exposed,[14] incorporation of deuterium is not expected to affect inhibitor potency. Indeed, the *in vitro* potencies of amlexanox (**1**) and d_2-amlexanox (**5**) against TBK1 are 0.6 ± 0.1 and 1.1 ± 0.3 µM, respectively (Figure 4 and Supplementary Materials Online). The difference is not statistically significant demonstrating that amlexanox can be deuterated without affecting inhibitor potency.

3.   CONCLUSIONS

As part of a program toward making analogues of amlexanox (**1**), which is being evaluated clinically for the treatment of type 2 diabetes and obesity, we decided to synthesize a derivative **5** to determine if placing deuterium at two sites of known metabolic activation of amlexanox might increase its half-life against three species of liver microsomes. Microsomes are rich in cytochrome (Cyp) P-450 enzymes, which are the major enzymes involved in drug metabolism

and account for about 75% of total metabolism.[22] The most common pathway of Cyp-mediated metabolism is hydroxylation of aliphatic carbons.

The data in Figure 3 show that amlexanox (**1**) and d_2-amlexanox (**5**) are relatively stable against all three liver microsomes ($t_{1/2}$ > 60 min) with amlexanox showing marginally greater stability relative to d_2-amlexanox except for rat liver microsomes. Hence, blocking two sites of metabolism with incorporation of a single deuterium on the C-7 methine carbon and another on a flanking methyl group of **5** does not majorly suppress Cyp-mediated metabolism relative to amlexanox. Metabolite identification experiments will be required to expand upon these findings. Additionally, synthetic chemistry needs to be developed that can specifically incorporate C-7 deuterium patterns (e.g., -CH(CH$_3$)(CH$_2$*D*) and -C*D*(CH$_3$)$_2$) aligned with known metabolites **2**-**4**, and additional patterns (e.g., -CH(C*D*$_3$)$_2$, -C*D*(C*D*$_3$)$_2$) to more fully explore the deuterium isotope effect.

4. EXPERIMENTAL

4.1 Materials and instrumentation. All starting monomers were obtained from commercial suppliers and were used without further purification. Routine ^{1}H NMR spectra were recorded at 400 or 500 MHz on a Varian 400 or 500 instrument, respectively, with CDCl$_3$ or DMSO-d_6 as solvent. Chemical shift values are recorded in δ units (ppm). High resolution mass spectrometry (HRMS) analysis was performed on an Agilent Q-TOF system. Analytical HPLC was performed on an Agilent 1100 series instrument with an Agilent Zorbax Eclipse Plus C18 (4.6 mm × 75 mm, 3.5 μm particle size) column with the gradient 10% acetonitrile/water (1 min), 10−90% acetonitrile/water (6 min), and 90% acetonitrile/water (2 min) flow = 1 mL/min. Thin-layer chromatography (TLC) was performed on silica gel GHLF plates (250 μm) purchased from Analtech. Column chromatography was carried out in the flash mode utilizing silica gel

(220−240 mesh) purchased from Silicycle. Extraction solutions were dried over anhydrous sodium sulfate prior to concentration.

4.2 Ethyl 2-amino-5-oxo-7-(prop-1-en-2-yl)-5*H*-chromeno[2,3-*b*]pyridine-3-carboxylate

(**7b**). A solution of tripotassium phosphate (2.63 g, 12.4 mmol) in water (6 mL) was added to a nitrogen-degassed suspension of ethyl 2-amino-7-bromo-5-oxo-5*H*-chromeno[2,3-*b*]pyridine-3-carboxylate[19] (**6**; 750 mg, 2.07 mmol), 4,4,5,5-tetramethyl-2-(prop-1-en-2-yl)-1,3,2-dioxaborolane (833 mg, 4.96 mmol), triphenylphosphine (271 mg, 1.03 mmol), Pd(OAc)$_2$ (60.3 mg, 0.27 mmol) in *p*-dioxane (60 mL) in a 500 mL RB flask. The mixture was heated at 100 -105 °C under nitrogen for 2 h. After cooling, the mixture was diluted with water (50 mL) and extracted with dichloromethane (2 x 120 mL). The combined organic phases were dried (Na$_2$SO$_4$) and concentrated to leave an orange solid that was triturated sequentially with small volumes of ethanol and ethyl ether, collected, and dried to leave **7b** (610 mg, 91%) as a white solid: mp 245-247 °C. ^{1}H NMR (400 MHz, chloroform-*d*): δ 9.16 (s, 1H), 8.38 (s, 1H), 8.31 (d, *J* = 2.3 Hz, 1H), 7.86 (dd, *J* = 8.8, 2.4 Hz, 1H), 7.47 (d, *J* = 8.7 Hz, 1H), 5.86 (s, 1H), 5.49 (d, *J* = 1.3 Hz, 1H), 5.23 - 5.18 (m, 1H), 4.41 (q, *J* = 7.1 Hz, 2H), 2.24 (dd, *J* = 1.5, 0.8 Hz, 3H), 1.45 (t, *J* = 7.1 Hz, 3H). HRMS: *m/z* (M+H)$^+$: calcd. for C$_{18}$H$_{16}$N$_2$O$_4$: 325.1183; Found, 325.1188.

4.3 Ethyl 2-amino-5-oxo-7-(propan-2-yl-1,2-*d*$_2$)-5*H*-chromeno[2,3-*b*]pyridine-3-carboxylate

(**8**). Tris(triphenylphosphine)rhodium(I) chloride (Wilkinson's catalyst; 339 mg, 0.366 mmol) was completely dissolved in anhydrous dichloromethane (10 mL) and ethanol-*d*$_1$ (10 mL) in a 250 mL 3-neck RB flask under nitrogen. The flask with the resulting clear red brown solution was evacuated by a water pump and then flushed with deuterium gas in a balloon. This flushing/evacuation procedure was repeated three more times, and then the mixture was stirred under deuterium gas (balloon pressure) for 20 min at room temperature. Then compound **7** (360 mg, 1.11 mmol) dissolved in a mixture of warm dichloromethane

(75 mL) and ethanol-d_1 (75 mL) was added by syringe. The resulting solution was stirred at room temperature for 4.5 h and then concentrated to a solid that was triturated in a small volume of benzene. The collected solids were further purified by flash silica gel column chromatography (elution with 0.5 - 1.0% methanol in dichloromethane). Product fractions were combined and concentrated to leave **8** (315 mg, 86%) as a while solid: mp 239-241 ºC. ^{1}H NMR (400 MHz, chloroform-d): δ 9.16 (s, 1H), 8.34 (s, 1H), 8.11 (d, J = 2.3 Hz, 1H), 7.59 (dd, J = 8.6, 2.3 Hz, 1H), 7.44 (d, J = 8.6 Hz, 1H), 5.84 (s, 1H), 4.41 (q, J = 7.1 Hz, 2H), 1.44 (t, J = 7.1 Hz, 3H), 1.30 (d, J = 6.5 Hz, 5H). HRMS: m/z (M+H)$^+$ Calcd. for C$_{18}$H$_{16}$D$_2$N$_2$O$_4$: 329.1465; Found 329.1480.

4.4 2-Amino-5-oxo-7-(propan-2-yl-1,2-d_2)-5H-chromeno[2,3-b]pyridine-3-carboxylic acid (d_2-amlexanox; 5). To a suspension of **8** (460 mg, 1.4 mmol) in ethanol (80 mL) and water (10 mL) was added 1 N aq. NaOH (10 mL) and the mixture was stirred at 50 °C for 90 min. TLC (5% methanol in dichloromethane) showed consumption of starting material. The mixture was filtered and the filtrate concentrated to a wet solid that dissolved in water (50 mL). The solution was acidified with 1 N aq. HCl to pH ~3 and the precipitated solids were stirred at room temperature for 20 h. After storage at room temperature for another 24 h, the solids were collected, washed with water, and dried under vacuum at 60 °C for 4 h to leave **5** (385 mg, 92%) as an off-white solid: mp > 300 ºC (dec.). ^{1}H NMR (500 MHz, DMSO-d_6): δ 13.45 (s, 1H), 8.80 (s, 1H), 8.25 (b, 2H), 7.92 (d, J = 2.3 Hz, 1H), 7.73 (dd, J = 8.6, 2.4 Hz, 1H), 7.53 (d, J = 8.6 Hz, 1H), 1.24 (d, J = 8.6 Hz, 5H). ^{13}C NMR (101 MHz, DMSO-d_6): δ 174.84, 167.35, 162.25, 161.46, 153.02, 144.93, 141.35, 133.71, 122.44, 120.91, 118.04, 106.23, 105.94, 33.70 – 31.07 (m), 23.64, 23.58 – 23.11 (m). HRMS: m/z (M+H)$^+$ Calcd. for C$_{16}$H$_{12}$D$_2$N$_2$O$_4$: 301.1152; Found 301.1157. HPLC: t_R, 6.42, purity 98.3%

4.5 Metabolic stability studies. The in vitro metabolism study of amlexanox and d_2-amlexanox were performed in human, rat and mice liver microsomes to evaluate the potential of

each compound for cytochrome P450-mediated metabolism. The metabolic stability was assessed as described using pooled CD-1 mouse liver microsomes, pooled SD rat liver microsmes and pooled human liver microsomes (purchased from Xeno Tech). 1 μM of each compound was incubated with 0.5 mg/mL liver microsomes and 1.7 mM cofactor β-NADPH in 0.1 M phosphate buffer (pH = 7.4) containing 3.3 mM $MgCl_2$ at 37 °C. The DMSO concentration was less than 0.1% in the final incubation mixture. At 0, 5, 10, 15, 30, 45, and 60 min of incubation, 40 μL of reaction mixture were removed and the reaction stopped immediately by adding 3-fold excess of cold acetonitrile containing 100 ng/mL of internal standard for quantification. The incubation without the addition of NADPH was used as a negative control. Verapamil were incubated similarly as a positive control substrate. The collected fractions were centrifuged at 15000 rpm for 10 min to collect the supernatant for LC−MS/MS analysis, from which the amount of remaining compound was determined. The natural log of the amount of compound remaining was plotted against time to determine the disappearance rate and the half-life of tested compounds. The LC−MS/MS method consisted of a Shimadzu HPLC system and chromatographic separation of tested compound was achieved using a Waters XBridge-C18 column (5 cm × 4.6 mm, 3.5 μm). An AB Sciex QTrap 5500 mass spectrometer equipped with an electrospray ionization source (Applied Biosystems, Toronto, Canada) in the negative-ion multiple reaction monitoring (MRM) mode for detection. The mobile phases were 0.1% formic acid in purified water (A) and 0.1% formic acid in acetonitrile (B). The gradient (B) was held at 10% (0-0.5 min), increased to 95% at 2 min, kept at isocratic 95% B for 1.0 min, and then immediately stepped back down to 10% for a 2 min re-equilibration. Flow rate was set at 1.0 mL/min. Amlexanox, d_2-amlexanox and internal standard 4-ASA were detected on the mass spectrometer by using multiple reaction monitoring transitions 297.1 → 253.2 *m/z*, 299.2 → 255.1 *m/z* and 152.0 → 108.0 *m/z*, respectively. Mass spectrometry parameter optimization was performed using an automated quantitative method provided by the manufacturer.

4.6   Kinase assay. The assay was performed as described previously.[15] Briefly, 50 nM purified TBK1 was incubated with 5 µM myelin basic protein and varying concentrations of inhibitor (from 10 µM to 0 µM). Reactions were initiated by the addition of 10 µM ATP spiked with [γ-^{32}P]-ATP and allowed to proceed for 30 min at room temperature. After quenching the reactions, radioactive phosphorylated substrate was quantified via phosphorimaging plates. Results were analyzed with GraphPad Prism 7 and fit to an inhibition dose-response sigmoidal curve with the Hill slope constrained to -1. Assays were repeated four independent times and the results reported as mean ± standard deviation. Statistical significance was determined via Student's two-tailed T-test ($p<0.05$).

ACKNOWLEDGMENTS

CONFLICT OF INTEREST

The authors report no conflicts of interest.

ORCID

Hollis Showalter; http://orcid.org/0000-0003-2863-0170

REFERENCES

1.   Giordano A, Frontini A, Cinti S. Convertible visceral fat as a therapeutic target to curb obesity. *Nat Rev Drug Discovery.* 2016;15(6):405-424.
2.   Saltiel AR. New therapeutic approaches for the treatment of obesity. *Science Translational Medicine.* 2016;8(323 323rv2):1-11.

3. Mowers J, Uhm M, Reilly SM, et al. Inflammation produces catecholamine resistance in obesity via activation of PDE3B by the protein kinases IKKε and TBK1. *eLife.* 2013;2:e01119/01111-01118.

4. Reilly SM, Saltiel AR. Adapting to obesity with adipose tissue inflammation. *Nat Rev Endocrinol.* 2017;13(11):633-643.

5. Chiang S-H, Bazuine M, Lumeng CN, et al. The protein kinase IKKε regulates energy balance in obese mice. *Cell (Cambridge, MA, U S).* 2009;138(5):961-975.

6. Saltiel AR. Insulin resistance in the defense against obesity. *Cell Metab.* 2012;15(6):798-804.

7. Clapham JC, Arch JRS. Targeting thermogenesis and related pathways in anti-obesity drug discovery. *Pharmacol Ther.* 2011;131(3):295-308.

8. Makino H, Saijo T, Ashida Y, Kuriki H, Maki Y. Mechanism of action of an antiallergic agent, amlexanox (AA-673), in inhibiting histamine release from mast cells. Acceleration of cAMP generation and inhibition of phosphodiesterase. *Int Arch Allergy Appl Immunol.* 1987;82(1):66-71.

9. Bell J. Amlexanox for the treatment of recurrent aphthous ulcers. *Clin Drug Invest.* 2005;25(9):555-566.

10. Oral EA, Reilly SM, Gomez AV, et al. Inhibition of IKKε and TBK1 improves glucose control in a subset of patients with type 2 diabetes. *Cell Metab.* 2017;26(1):157-170.e157.

11. Torii H, Yoshida K, Tsukamoto T, et al. Metabolic fate of amoxanox (AA-673), a new antiallergic agent, in rats, mice, guinea pigs and dogs. *Yakuri to Chiryo.* 1985;13(9):4933-4954.

12. Yoshida K, Danayama K. Pharmacokinetics and metabolism of amlexanox (AA-673), a new antiallergic agent, after nasal administration to rats. *Yakuri to Chiryo.* 1987;15(5):1873-1881.

13. Ukawa K, Ishiguro T, Kuriki H, Nohara A. Synthesis of the metabolites and degradation products of 2-amino-7-isopropyl-5-oxo-5*H*-[1]benzopyrano[2,3-*b*]pyridine-3-carboxylic acid (amoxanox). *Chem Pharm Bull.* 1985;33(10):4432-4437.

14. Beyett TS, Gan X, Reilly SM, et al. Carboxylic acid derivatives of amlexanox display enhanced potency toward TBK1 and IKKε and reveal mechanisms for selective inhibition. *Mol Pharmacol.* 2018;94(4):1210-1219.

15. Beyett TS, Gan X, Reilly SM, et al. Design, synthesis, and biological activity of substituted 2-amino-5-oxo-5*H*-chromeno[2,3-*b*]pyridine-3-carboxylic acid derivatives as inhibitors of the inflammatory kinases TBK1 and IKKε for the treatment of obesity. *Bioorg Med Chem.* 2018;26(20):5443-5461.

16. Shao L, Hewitt MC. The kinetic isotope effect in the search for deuterated drugs. *Drug News Perspect.* 2010;23(6):398-404.

17. Saltiel AR, Showalter HD, Larsen S. Preparation of deuterated amlexanox derivatives for use as TBK1 or IKKε protein kinase inhibitors. US Patent 9,944,652, Apr. 17, 2018.

18. Nishimura S. *Handbook of Heterogeneous Catalytic Hydrogenation for Organic Synthesis.* New York: John Wiley & Sons; 2001. Chapter 3, pp. 68-72.

19. Ghosh C, Sinharoy DK, Mukhopadhyay KK. Heterocyclic systems. Part 6. Reactions of 4-oxo-4*H*-[1]benzopyran-3-carbonitriles with hydrazine, phenylhydrazine, hydroxylamine, and some reactive methylene compounds. *J Chem Soc, Perkin Trans 1.* 1979(8):1964-1968.

20. Rakoff H. Preparation of fatty acids and esters containing deuterium. *Prog Lipid Res.* 1982;21(3):225-254.

21. Lie Ken Jie MSF, Choi YC. Mass spectral studies of deuterium-labeled picolinyl fatty esters in the determination of double-bond positions. *J Am Oil Chem Soc.* 1992;69(12):1245-1247.

22. Guengerich FP. Cytochrome P450 and chemical toxicology. *Chem Res Toxicol.* 2008;21(1):70-83.

SUPPORTING INFORMATION

Additional Supporting Information may be found online in the supporting information tab for this article (^{1}H NMR and high resolution mass spectra data for compounds **1**, **5**, **7a** and **8**, ^{13}C NMR spectra for **1** and **5**, HPLC for **5**, and gels from radiometric kinase assays for **1** and **5**).

A derivative of the TBK1 inhibitor amlexanox (**1**) has been synthesized with deuterium introduced into two sites of metabolism on the C-7 isopropyl function. d_2-Amlexanox (**5**) displayed nearly equivalent potency to amlexanox (IC_{50} 1.1 μM vs 0.6 μM, respectively) against recombinant human TBK1. When incubated with human, rat, and mouse liver microsomes, **1** and **5** were stable ($t_{1/2}$ > 60 minutes) with **1** showing marginally greater stability relative to **5** except for rat liver microsomes.

amlexanox (**1**)

sites of metabolism
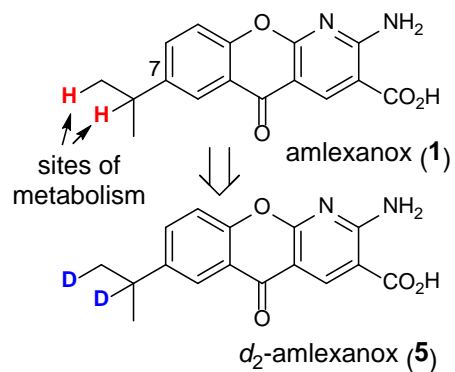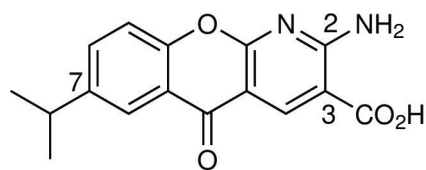
d_2-amlexanox (**5**)

amlexanox
(**1**)
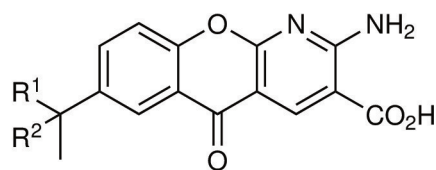
2: R^1 = CH$_3$; R^2 = OH
3: R^1 = CH$_2$OH; R^2 = H
4: R^1 = CO$_2$H; R^2 = H

5

jlcr_3716_f1.eps

Amlexanox (**1**)

H (p)
3.05

I (d)
1.25

*d*₂-Amlexanox (**5**)
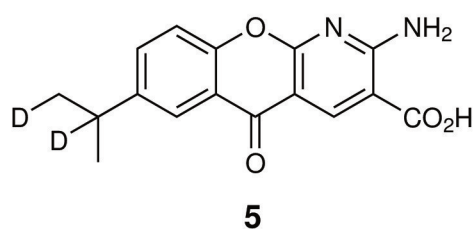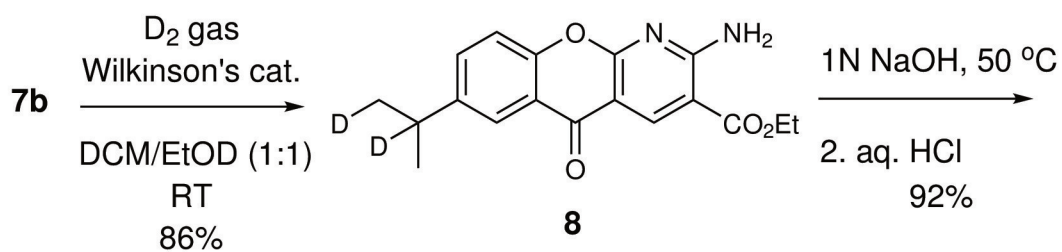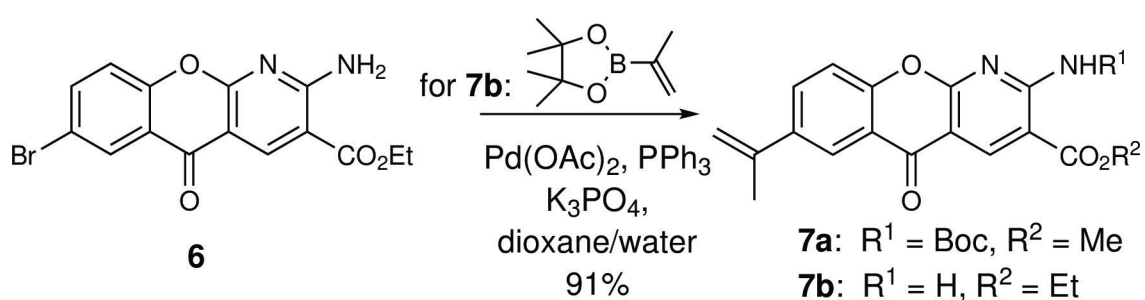
G (d)
1.24

1.02

6.48

5.07

3 2 1

3 2 1
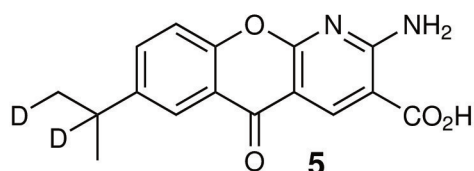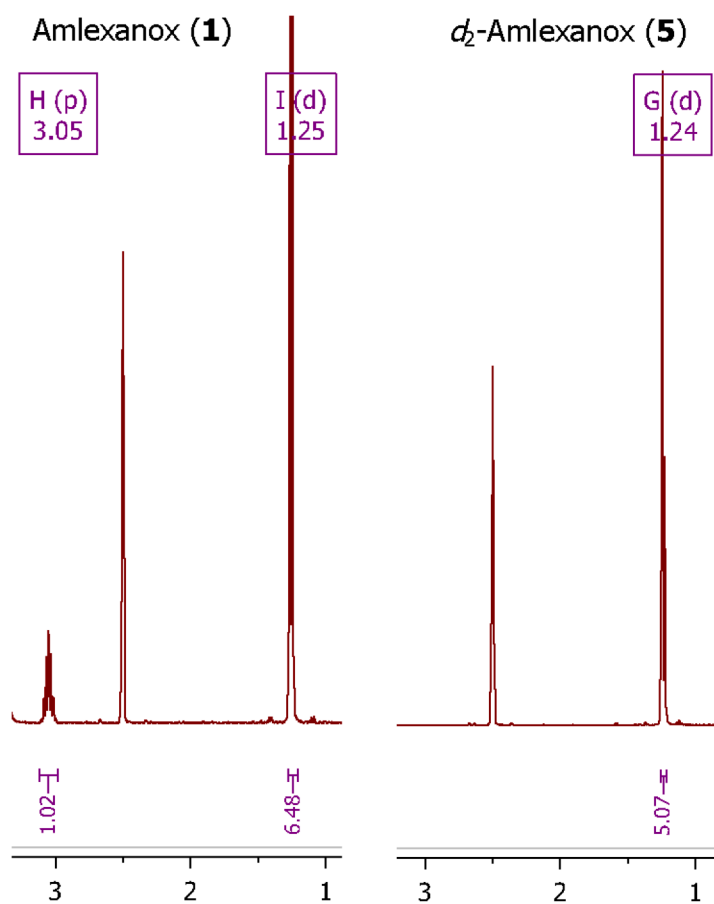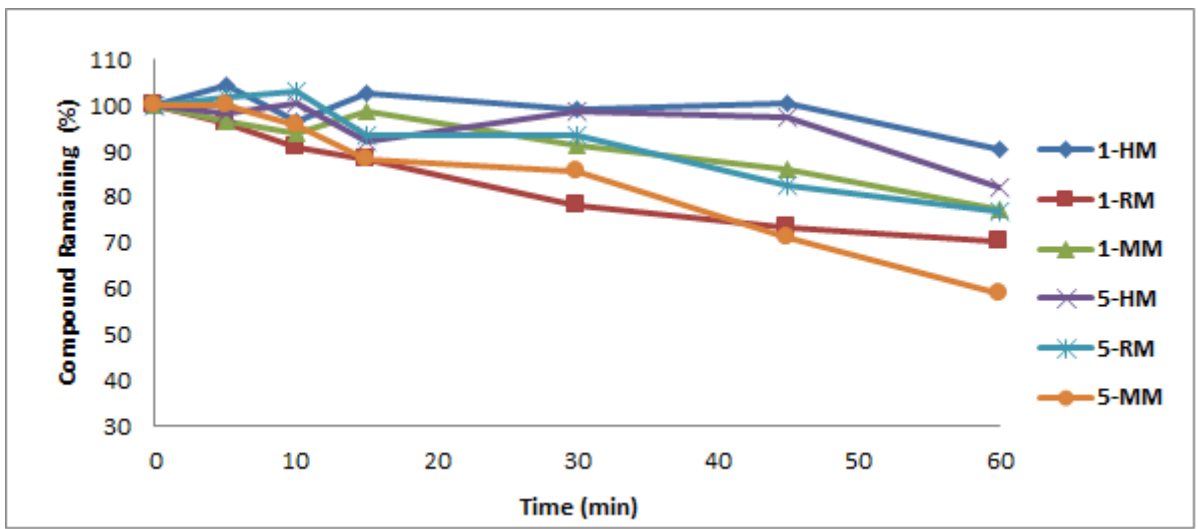
JLCR_3716_f2.tiff

JLCR_3716_f3.tif
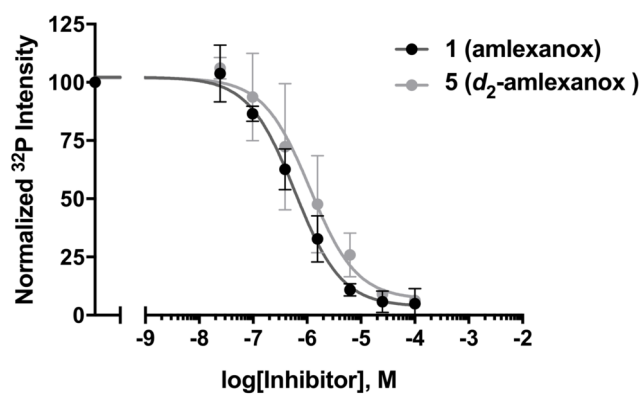
JLCR_3716_f4.tiff

jlcr_3716_scheme 1.eps